ACADEMIC PRESS

Available online at www.sciencedirect.com

SCIENCE DIRECT®

DEVELOPMENTAL BIOLOGY

Developmental Biology 261 (2003) 506–519

www.elsevier.com/locate/ydbio

Cell-autonomous and nonautonomous actions of endothelin-A receptor signaling in craniofacial and cardiovascular development

David E. Clouthier,[a,b,1] S. Clay Williams,[a,b] Robert E. Hammer,[a,c] James A. Richardson,[d,e] and Masashi Yanagisawa[a,b,e,*]

[a] *Howard Hughes Medical Institute, University of Texas Southwestern Medical Center, 5323 Harry Hines Boulevard, Dallas, TX 75390, USA*
[b] *Department of Molecular Genetics, University of Texas Southwestern Medical Center, 5323 Harry Hines Boulevard, Dallas, TX 75390, USA*
[c] *Department of Biochemistry, University of Texas Southwestern Medical Center, 5323 Harry Hines Boulevard, Dallas, TX 75390, USA*
[d] *Department of Pathology, University of Texas Southwestern Medical Center, 5323 Harry Hines Boulevard, Dallas, TX 75390, USA*
[e] *The Donald W. Reynolds Cardiovascular Clinical Research Center, University of Texas Southwestern Medical Center, 5323 Harry Hines Boulevard, Dallas, TX 75390, USA*

Received for publication 28 November 2001, revised 21 February 2003, accepted 24 February 2003

Abstract

Craniofacial and cardiac development relies on the proper patterning of the neural crest-derived ectomesenchyme of the pharyngeal arches, from which many craniofacial and great vessel structures arise. One of the intercellular signaling molecules that is involved in this process, endothelin-1 (ET-1), is expressed in the arch epithelium and influences arch development by binding to its cognate receptor, the endothelin A (ET_A) receptor, found on ectomesenchymal cells. We have previously shown that absence of ET_A signaling in $ET_A^{-/-}$ mouse embryos disrupts neural crest cell development, resulting in craniofacial and cardiovascular defects similar in many aspects to those in mouse models of DiGeorge syndrome. These changes may reflect a cell-autonomous requirement for ET_A signaling during crest cell development because the ET_A receptor is an intracellular signaling molecule. However, it is also possible that some of the observed defects in $ET_A^{-/-}$ embryos could arise from the absence of downstream signaling that act in a non-cell-autonomous manner. To address this question, we performed chimera analysis using $ET_A^{-/-}$ embryonic stem cells. We observe that, in almost all early $ET_A^{-/-} \leftrightarrow {}^{+/+}$ chimeric embryos, $ET_A^{-/-}$ cells are excluded from the caudoventral aspects of the pharyngeal arches, suggesting a cell-autonomous role for ET_A signaling in crest cell migration and/or colonization. Interestingly, in the few embryos in which mutant cells do reach the ventral arch, structures derived from this area are either composed solely of wild type cells or are missing, suggesting a second cell-autonomous role for ET_A signaling in postmigratory crest cell differentiation. In the cardiac outflow tract and great vessels, $ET_A^{-/-}$ cells are excluded from the walls of the developing pharyngeal arch arteries, indicating that ET_A signaling also acts cell-autonomously during cardiac neural crest cell development.

Keywords: Neural crest cell; Pharyngeal arch; Chimera; Mouse; Craniofacial; Cardiovascular

Introduction

The development of most of the bone and cartilage of the jaw and throat, as well as the cardiac outflow tract and aortic arch, relies on neural crest cells (Kirby et al., 1983, 1985; Le Lievre and Le Douarin, 1975; Noden, 1983). These cells originate from the posterior midbrain and hindbrain, migrate to the pharyngeal arches (Lumsden et al., 1991; Serbedzija et al., 1992) and arch arteries (Kirby et al., 1983; Kirby and Stewart, 1983), and subsequently contribute to the formation of mature structures of the head and heart (Creazzo et al., 1998; Kontges and Lumsden, 1996; Le Douarin et al., 1993). The development of neural crest cells is regulated by a number of factors expressed by the over-

* Corresponding author. Fax: +1-214-648-5068.
E-mail address: Masashi.Yanagisawa@UTSouthwestern.edu (M. Yanagisawa).
[1] Present Address: Department of Molecular, Cellular and Craniofacial Biology, Birth Defects Center, University of Louisville, Louisville, KY 40292.

0012-1606/03/$ – see front matter © 2003 Elsevier Inc. All rights reserved.
doi:10.1016/S0012-1606(03)00128-3

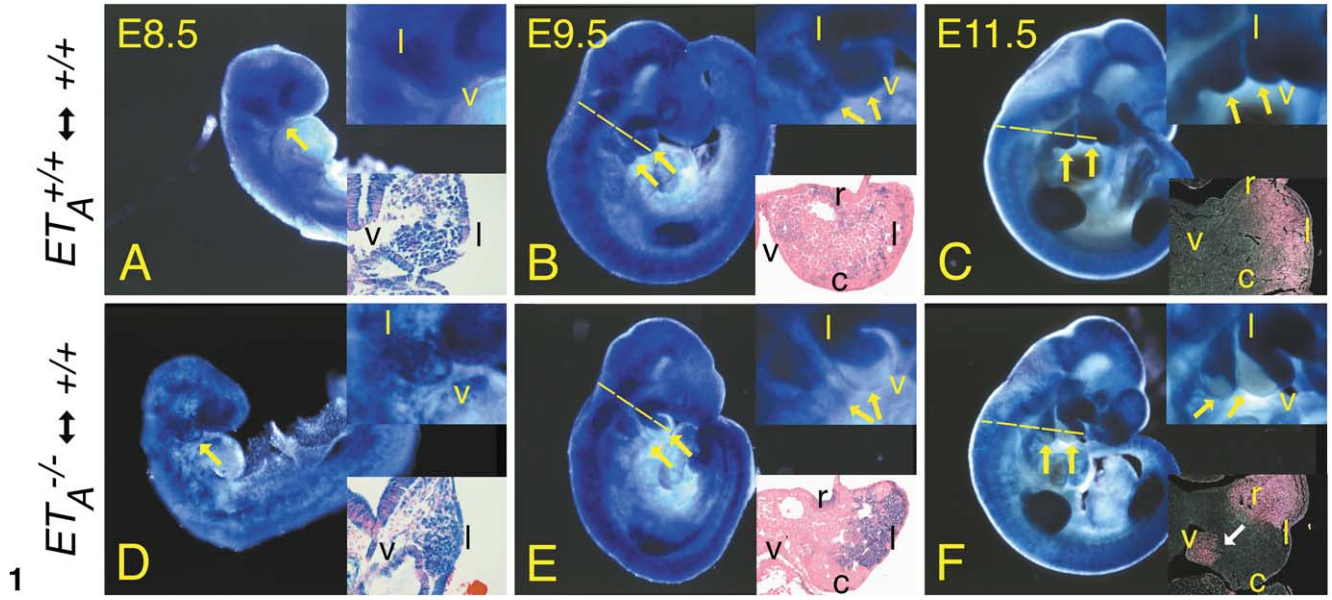
E8.5
E9.5
E11.5
$ET_A^{+/+} \leftrightarrow +/+$
$ET_A^{-/-} \leftrightarrow +/+$
A
B
C
D
E
F
l
v
r
c

1

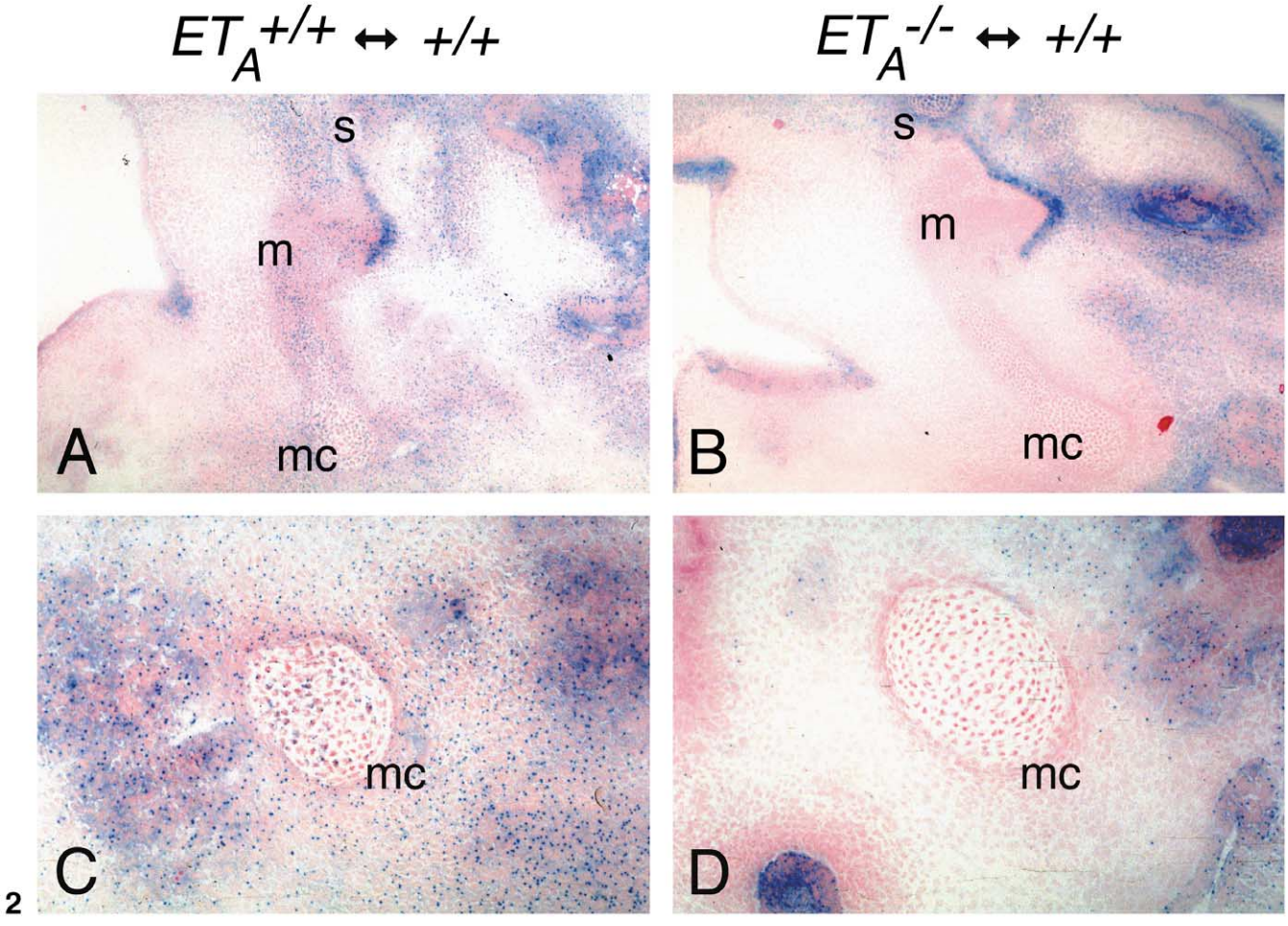
$ET_A^{+/+} \leftrightarrow +/+$
$ET_A^{-/-} \leftrightarrow +/+$
s
m
mc
A
B
C
D

2

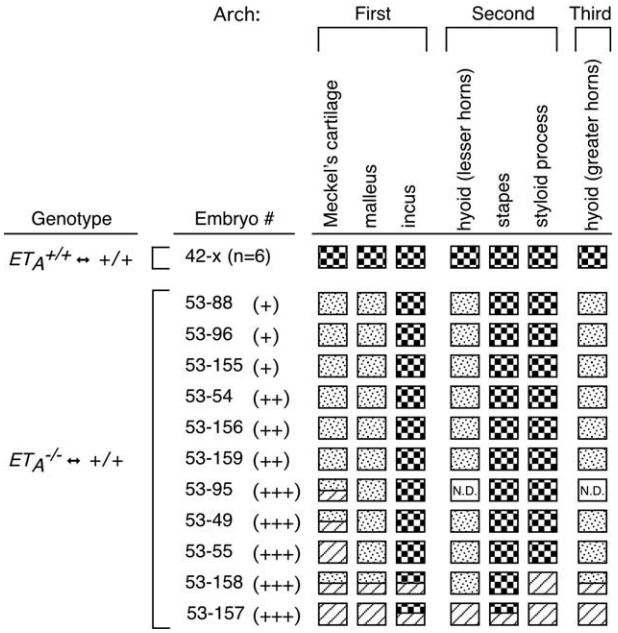

Fig. 3. Contribution of $ET_A^{+/+}$ or $ET_A^{-/-}$ cells to craniofacial structure of E13.5 chimeric embryos. Structures examined are listed along the top, as well as their arch of origin. The genotype of the embryos is listed along the left. Because the phenotype of the $ET_A^{+/+}\leftrightarrow+/+$ chimeras was the same in each chimera examined, all six were combined. For $ET_A^{-/-}\leftrightarrow+/+$ chimeras, the relative chimerism is listed in parenthesis next to the embryo number: +, 1–33% contribution of injected cells; ++, 34–66% contribution of injected cells; +++, 67–100% contribution of injected cells. ▩, structures composed of both injected and recipient cells; ▨, structures composed of recipient cells only; ▧, structures that are absent. While all structures in $ET_A^{+/+}\leftrightarrow+/+$ chimeras are composed of both $ET_A^{+/+}$ and recipient wild type cells, ventral structures (Meckel's cartilage, malleus and lessor horns of the hyoid) in $ET_A^{-/-}\leftrightarrow+/+$ chimeras are composed of wild type cells only. In $ET_A^{-/-}\leftrightarrow+/+$ chimeras containing a high percentage of $ET_A^{-/-}$ cells, these ventral structures are absent. More lateral structures (incus, stapes and styloid) are composed of both $ET_A^{-/-}$ and recipient wild type cells; like the ventral structures, these elements are absent in chimeras containing a high percentage of mutant cells.

lying arch epithelium and arch artery endothelium. Endothelin-1 (ET-1) is expressed by ectodermal and endodermal arch epithelium, as well as by the paraxial mesoderm-derived arch core, and has been hypothesized to be a crucial factor in establishing rostral–caudal arch polarity of the first mandibular arch (Tucker et al., 1999).

Inactivation of genes encoding ET-1 (Kurihara et al., 1994), the endothelin-A (ET_A) receptor (Clouthier et al., 1998) (the primary receptor for ET-1 on cephalic crest cells), and endothelin converting enzyme (ECE-1) (the essential protease for the biosynthesis of ET-1; Yanagisawa et al., 1998a) all result in specific defects in craniofacial and cardiovascular structures derived from cephalic and cardiac neural crest cells. Many of these defects overlap with those found in patients with DiGeorge (velo-cardiofacial) syndrome and its recently described mouse models (Jerome and Papaioannou, 2001; Lindsay et al., 2001; Merscher et al., 2001; Kochilas et al., 2002; Vitelli et al., 2002). Craniofacial defects associated with loss of endothelin signaling are most pronounced in ventral arch derivatives and reflect the arch area in which ET_A signaling is crucial for initiating or maintaining expression of multiple transcription factors (Clouthier et al., 2000). However, craniofacial defects in $ET_A^{-/-}$ embryos are not confined to the derivatives of the ventral half, suggesting either that ET_A signaling can influence lateral arch patterning through other paracrine mediators or that these defects occur as a secondary event to the ventral defects.

ET_A receptor signaling also plays a critical role in cardiac neural crest cell development (Clouthier et al., 1998; Kurihara et al., 1994; Yanagisawa et al., 1998a,b). We previously showed that ET_A receptor signaling by the crest-derived mesenchymal cells that normally surround the arch arteries is crucial for correct remodeling of arch arteries 4 and 6 (Clouthier et al., 1998; Yanagisawa et al., 1998b). However, defects in remodeling of arch artery 3 were not observed, suggesting that ET_A receptor signaling is necessary only for the development of arch arteries 4 and 6 or that in arch arteries 3, it can be compensated for by other factors. It is also possible that ET_A action is required by all arch arteries, but structural defects can only be detected in arteries 4 and 6.

Fig. 1. Contribution of ET_A wild type and mutant cells to the developing pharyngeal arches of chimeric embryos. Whole-mount β-galactosidase staining of $ET_A^{+/+}\leftrightarrow+/+$ (A–C) and $ET_A^{-/-}\leftrightarrow+/+$ mutant (D–F) chimeras are shown at E8.5 (A, D), E9.5 (B, E), and E11.5 (C, F). Upper insets show a magnification of the pharyngeal arch region; the lower insets show transverse sections through the left mandibular arch of the embryos; sections are counterstained with eosin. To aid in visualization, lower insets in (C) and (F) are shot in dark field, resulting in β-gal staining appearing pink. For orientation purposes, lateral (l), ventral (v), rostral (r), and caudal (c) aspects of the mandibular arch are denoted. At E8.5, no obvious differences are observed in cell distribution between $ET_A^{+/+}\leftrightarrow+/+$ (A) and $ET_A^{-/-}\leftrightarrow+/+$ chimeric (D) embryos. However, at both E9.5 and E11.5, $ET_A^{-/-}$ cells (blue) are excluded from the caudoventral aspects of the arches of $ET_A^{-/-}\leftrightarrow+/+$ chimeras (yellow arrows), with ventral aspects composed almost solely of wild type (unstained) cells (E, F). In a few $ET_A^{-/-}\leftrightarrow+/+$ chimeras, scattered clumps of $ET_A^{-/-}$ cells are observed in more ventral regions (white arrow in lower inset in F). In contrast, $ET_A^{+/+}$ cells (blue) are found throughout the arches of $ET_A^{+/+}\leftrightarrow+/+$ chimeras and are mixed homogeneously with wild type (unstained) cells (B, C). The distribution of $ET_A^{-/-}$ cells was unchanged in other regions of $ET_A^{-/-}\leftrightarrow+/+$ chimeras.

Fig. 2. Development of craniofacial structures in E13.5 chimeric embryos. Transverse sections from $ET_A^{+/+}\leftrightarrow+/+$ (A, C) and $ET_A^{-/-}\leftrightarrow+/+$ (B, D) chimeras stained for β-galactosidase activity (blue) and counterstained with eosin (pink). (A, B) Sections through the middle ear region. In $ET_A^{+/+}\leftrightarrow+/+$ chimeras, $ET_A^{+/+}$ cells (blue) are observed in the malleus (m) and Meckel's cartilage (mc) (and the surrounding mesenchyme), as well as the stapes (s), and are mixed homogeneously with wild type (pink) cells (A). In contrast, $ET_A^{-/-}$ cells (blue) in $ET_A^{-/-}\leftrightarrow+/+$ chimeras are only observed in the stapes (B). The malleus and Meckel's cartilage are composed only of wild type cells (pink). (C, D) Sections through the distal aspects of Meckel's cartilage. While $ET_A^{+/+}$ cells in $ET_A^{+/+}\leftrightarrow+/+$ chimeras are observed in and surrounding Meckel's cartilage (C), $ET_A^{-/-}$ cells in $ET_A^{-/-}\leftrightarrow+/+$ chimeras are absent from both Meckel's cartilage and the surrounding perichondrium (D).

The use of chimeras, in which mutant cells are mixed with wild type cells and their involvement in development subsequently followed, can help define whether a gene acts in a cell-autonomous or non-cell-autonomous manner (Rossant and Spence, 1998). Several chimera analyses have been performed to examine the role of different genes in pharyngeal arch and cardiac development (Chen and Behringer, 1995; Rivera-Perez et al., 1999; Tran and Sucov, 1998). To better understand the role of ET_A signaling in the development of individual craniofacial elements and the cardiac outflow tract, we have undertaken chimera analysis using $ET_A^{-/-}$ ES cells. We find that $ET_A^{-/-}$ cells are almost always excluded from the caudoventral pharyngeal arches of $ET_A^{-/-} \leftrightarrow {}^{+/+}$ chimeras during arch development in a pattern consistent with a cell-autonomous requirement for ET_A signaling during neural crest cell migration. Examination of older embryos illustrates that most elements derived from the ventral aspects of mandibular arch one and arch two, including the mandible and Meckel's cartilage, are either composed solely of wild type cells or are absent, regardless of whether any mutant cells reach the ventral arch. In contrast, elements derived from the lateral aspects of both the maxillary part of arch one and arch two, including the incus and stapes, are composed of both wild type and mutant cells. These findings suggest a second cell-autonomous requirement for ET_A signaling during neural crest cell differentiation in the ventral arch. In the cardiac outflow tract, $ET_A^{-/-}$ cells are excluded from the walls of arch arteries 3, 4, and 6, suggesting that ET_A signaling is also required in a cell-autonomous manner by cardiac neural crest cells during their development.

Materials and methods

Generation and maintenance of $ET_A^{+/-}$ mice

The targeted disruption of the ET_A allele was previously described (Clouthier et al., 1998). Briefly, exons 5 and 6, encoding the sixth and seventh transmembrane spanning domains of the ET_A receptor, were replaced with a targeting vector through homologous recombination. $ET_A^{+/-}$ mice were maintained on a 129S6/SvEv background and genotyped by PCR (Clouthier et al., 1998). For generation of ES cells, $ET_A^{+/-}$ mice were bred with *ROSA26* hemizygous mice obtained from The Jackson Laboratories. These mice carry an insertion vector containing a *lacZ* gene, which is ubiquitously expressed in all embryonic tissues throughout development (Friedrich and Soriano, 1991). Mice were genotyped for the *ROSA26* insertion by using a three primer PCR that delineates wild type, hemizygous, and homozygous *ROSA26* mice. The mutant allele is amplified by using primers F150 (5′-GGCTTAAAGGCTAACCTGATGTG-3′) and R1295 (5′-GCGAAGAGTTTGTCCTCAACC-3′), which amplifies an 1146-bp product. The wild type allele is amplified with F150 and R523 (5′-GGAGCGGGAGAAATGGATATG-3′), which amplifies a 374-bp product.

Production of $ET_A^{-/-}$ ES cells

ES cell lines were generated from delayed blastocysts obtained from matings between $ET_A^{+/-}$; *ROSA26*$^{+/-}$ mice by using previously described methods (Robertson, 1987). Cell lines were genotyped for the ET_A allele by both PCR and Southern blot analyses, and for the *ROSA26* allele by PCR.

Generation and characterization of ET_A chimeras

$ET_A^{+/+}$, $^{+/-}$, or $^{-/-}$ ES cells (all of which also contained the *ROSA26* insertion vector) at passage 3–6 were injected into blastocysts obtained from C57BL6/J female mice. Chimeric embryos examined at E8.5, E9.5, and E11.5 were collected into phosphate-buffered saline (PBS, Life Technologies), fixed in 4% paraformaldehyde for 1 h at 4°C and then stained for β-galactosidase activity as previously described (Zambrowicz et al., 1994). After staining, embryos were rinsed in PBS, processed into paraffin, and sectioned transversely at 5 μm. Chimeric embryos examined at E13.5 and E18.5 were first embedded in OCT freezing media (Tissue-Tek) and snap frozen. A Leica cryostat was then used to cut 14-μm sections, which were collected onto poly-L-lysine slides (Histology Control Systems), air dried, fixed in 0.5% gluteraldehyde for 20 min, rinsed, and then stained for β-galactosidase activity overnight at 37°C. After rinsing in PBS, slides were lightly counterstained with eosin before coverslipping with PBX mounting media (BDH Laboratory Chemicals). For all of these analyses, X-gal (Pharmacia) was used as the substrate for β-galactosidase.

Analysis of β-galactosidase staining

To grossly determine the overall contribution of injected ES cells in E13.5 and E18.5 chimeric embryos, six consecutive sections in both the head and heart regions were examined. In E18.5 embryos, this was further confirmed by analyzing β-galactosidase staining in trunk skin. To do this, back trunk skin was removed prior to embryo embedding, spread onto a small piece of 3MM Whatman paper, fixed in 0.5% gluteraldehyde for 20 min at 4°C, rinsed in PBS, and stained for β-galactosidase overnight at 37°C.

Bone and cartilage staining

E18.5 $ET_A^{+/+} \leftrightarrow {}^{+/+}$ and $ET_A^{-/-} \leftrightarrow {}^{+/+}$ embryos were collected and processed for bone and cartilage staining by using alizarin red and alcian blue, respectively, as previously described (Clouthier et al., 1998).

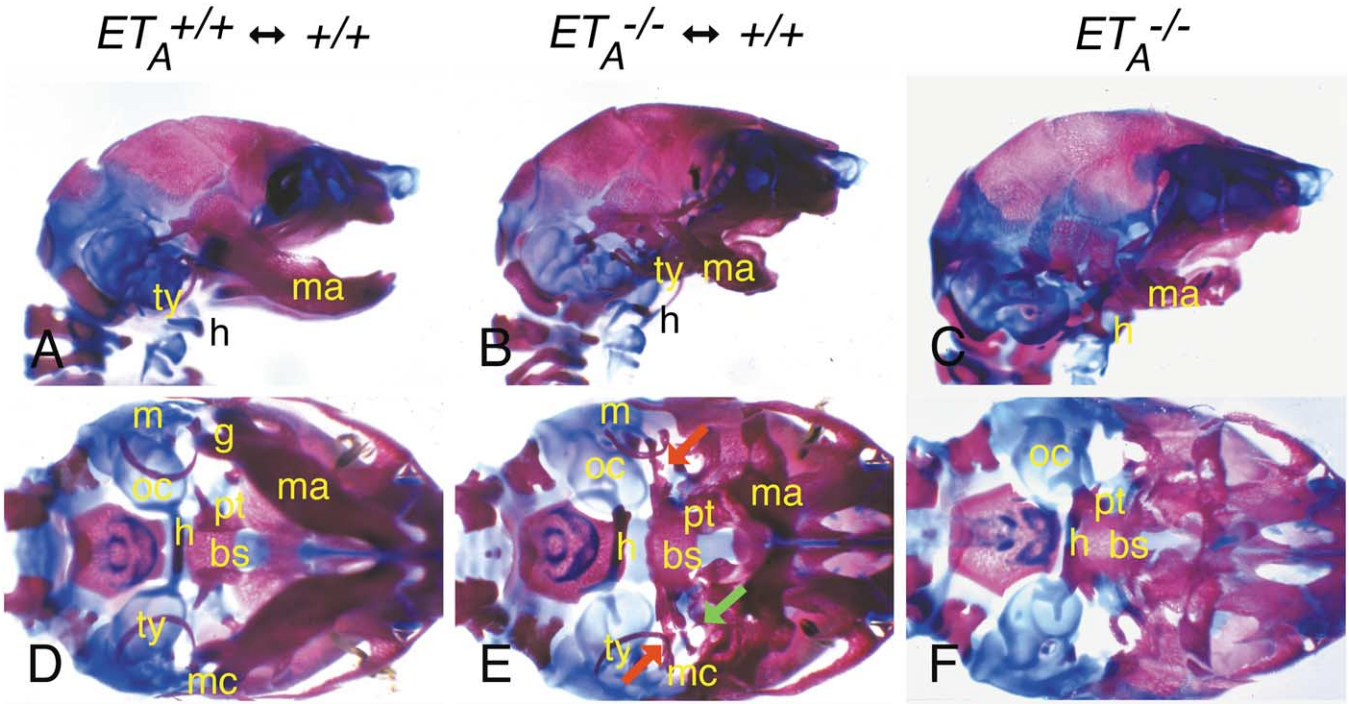

Fig. 4. Skeletal analysis of craniofacial structures in E18.5 chimeric embryos. Lateral (A–C) and ventral (D–F) views of the skulls of $ET_A^{+/+}\leftrightarrow+/+$ chimeras (A, D), $ET_A^{-/-}\leftrightarrow+/+$ chimeras (B, E) and $ET_A^{-/-}$ embryos (C, F) stained with alizarin red and alcian blue. Numerous changes are observed in neural crest-derived skull elements in $ET_A^{-/-}\leftrightarrow+/+$ chimeras (B, E), representing an intermediate phenotype between $ET_A^{+/+}\leftrightarrow+/+$ chimeras and ET_A mutant embryos. These changes include truncation of Meckel's cartilage (mc; green arrow), reduction in mandible (ma) size and organization, abnormal lessor horns of the hyoid (h), and asymmetrical reduction in tympanic ring (ty) size. Red arrows in (E) point to the struts that form between the gonial (g) and pterygoid (pt) bones. bs, basisphenoid; m, malleus; oc, otic capsule.

Results

To examine the cell-autonomous nature of ET_A receptor signaling during craniofacial and cardiovascular development, we created chimeric embryos containing a mixture of wild type and $ET_A^{-/-}$ cells. To accomplish this, we first bred $ET_A^{+/-}$ mice with mice from the *ROSA26* line; these mice carry a *lacZ* insertion vector that is ubiquitously expressed throughout development (Friedrich and Soriano, 1991). Crossing *ROSA26* onto the $ET_A^{+/-}$ background allowed us subsequently to follow both $ET_A^{+/+}$ and $ET_A^{-/-}$ cells in chimeric embryos by staining for β-galactosidase (β-gal) activity. ES cells were isolated from delayed blastocysts obtained from matings of $ET_A^{+/-}$;$ROSA26^{+/-}$ mice, with 68 plated blastocysts giving rise to 17 ES cell lines, 2 of which were $ET_A^{-/-}$;$ROSA26^{+/-}$ and 2 of which were $ET_A^{+/+}$; $ROSA26^{+/-}$ (data not shown). This method of ES cell isolation provided low passage ES cell lines for injection, thus reducing the chance of ES cell differentiation. Both $ET_A^{-/-}$; $ROSA26^{+/-}$ cell lines (clones 53 and 75) were injected into wild type blastocysts, giving rise to $ET_A^{-/-}\leftrightarrow{}^{+/+}$ mutant chimeric embryos. As similar patterns were observed in $ET_A^{-/-}\leftrightarrow{}^{+/+}$ chimeras at E9.5 and E10.5 using either of these clones, we focused the bulk of our analysis on clone 53. One $ET_A^{+/+}$;$ROSA26^{+/-}$ cell line (clone 42) was injected into wild type blastocysts to produce $ET_A^{+/+}\leftrightarrow{}^{+/+}$ control chimeras. One $ET_A^{+/-}$;$ROSA26^{+/-}$ cell line (clone 74) was also injected as a control and gave the same results as the $ET_A^{+/+}$; $ROSA26^{+/-}$ cells (data not shown). A total of 737 blastocysts were injected, 397 embryos of varying ages collected, of which 288 were chimeric. The extent of chimerism ranged from $<5\%$ to $>95\%$, with a mean of $\approx50\%$ (data not shown).

Segregation of ET_A mutant cells in the pharyngeal arches

We first examined the contribution of $ET_A^{-/-}$ cells in early $ET_A^{-/-}\leftrightarrow{}^{+/+}$ chimeras using whole-mount β-gal staining. Since $ET_A^{-/-}$ embryos have numerous craniofacial defects that apparently arise from aberrant neural crest cell development, we focused our analysis on pharyngeal arch development. We initially examined E8.5, E9.5, and E11.5 embryos because this time period would encompass both crest migration away from the neural tube and initial differentiation once in the pharyngeal arches (Chai et al., 2000; Lumsden et al., 1991; Serbedzija et al., 1992). Embryos were collected, fixed, stained for β-gal activity, and serially sectioned.

At E8.5, no detectable differences were noted between $ET_A^{+/+}\leftrightarrow{}^{+/+}$ and $ET_A^{-/-}\leftrightarrow{}^{+/+}$ chimeric embryos, with $ET_A^{+/+}$ and $ET_A^{-/-}$ cells contributing equally to all tissues (blue cells in Fig. 1A and D). This included the first arch, where transverse sections confirmed this mixing (lower insets, Fig. 1A and D). Differences were also not observed in $ET_A^{+/+}\leftrightarrow{}^{+/+}$ chimeras at E9.5 (Fig. 1B) or E11.5 (Fig.

1C), in which $ET_A^{+/+}$ and wild type cells were mixed in a homogenous pattern throughout the arches. However, in E9.5 (Fig. 1E) and E11.5 (Fig. 1F) $ET_A^{-/-} \leftrightarrow {}^{+/+}$ chimeric embryos, $ET_A^{-/-}$ cells were excluded from a caudoventral wedge in the first and second arches, with this region instead being composed almost solely of unstained wild type cells (compare yellow arrows in Fig. 1B and C and E and F). Mutant cells were observed in more rostrolateral regions of the arch, and β-gal staining in this region appeared darker than in control chimeras. This was further apparent in transverse sections through the first arch (compare lower insets in Fig. 1B and C and E and F). This segregation was observed in 35/37 $ET_A^{-/-} \leftrightarrow {}^{+/+}$ embryos examined at E9.5 and 25/27 $ET_A^{-/-} \leftrightarrow {}^{+/+}$ embryos examined at E11.5. Further, the degree of segregation was inversely related to the extent of mutant cell contribution: as the contribution of $ET_A^{-/-}$ cells in the chimera increased, this sharp $ET_A^{-/-}$ boundary extended further in a caudoventral direction (data not shown). Two $ET_A^{-/-} \leftrightarrow {}^{+/+}$ chimeras, in which the contribution of $ET_A^{-/-}$ cells was greater than 90%, had blue cells at the ventral most aspects of the arches (data not shown). From these findings, it appears that wild type cells either have an advantage reaching the ventral arch or proliferating once there.

Contribution of $ET_A^{-/-}$ cells to arch derived structures in mutant chimeras

We next examined the contribution of $ET_A^{+/+}$ and $ET_A^{-/-}$ cells to developing craniofacial structures in E13.5 $ET_A^{+/+} \leftrightarrow {}^{+/+}$ and $ET_A^{-/-} \leftrightarrow {}^{+/+}$ chimeras by examining β-gal activity in transverse frozen sections. In $ET_A^{+/+} \leftrightarrow {}^{+/+}$ chimeras, $ET_A^{+/+}$ cells (blue) were observed throughout structures derived from the maxillary arch (incus), mandibular arch (Meckel's cartilage and the malleus), and second arch (stapes) ($n = 6$) (Figs. 2A and 3). In contrast, $ET_A^{-/-}$ cells (blue) in $ET_A^{-/-} \leftrightarrow {}^{+/+}$ chimeras were conspicuously absent from the malleus and Meckel's cartilage, as well as in the surrounding head and jaw mesenchyme ($n = 11$) (Figs. 2B and 3). This area was instead composed of wild type cells (pink). Mutant cells were also not observed in the lessor horns of the hyoid bone. This lack of contribution was independent of the percentage of mutant cells present. More importantly, in $ET_A^{-/-} \leftrightarrow {}^{+/+}$ chimeras containing a large percentage of mutant cells, these structures were absent (Fig. 3). However, $ET_A^{-/-}$ cells were always mixed in a homogenous pattern with wild type cells in the incus and stapes (Figs. 2B and 3). It thus appears that $ET_A^{-/-}$ cells cannot contribute to structures derived from the mandibular arch or ventral second arch, but can participate in the formation of structures derived from the maxillary arch and lateral second arch in the presence of wild type cells.

Structural analysis of skull elements

The inability of mutant cells to contribute to ventral arch elements in E13.5 $ET_A^{-/-} \leftrightarrow {}^{+/+}$ chimeric embryos suggested the possibility that the development of these ventral elements could be adversely affected in $ET_A^{-/-} \leftrightarrow {}^{+/+}$ chimeric embryos with a high percentage of mutant cells. To investigate this point, we examined arch-derived bone and cartilage structures of the head of E18.5 embryos using alizarin red and alcian blue staining. As expected, we observed defects in numerous structures of $ET_A^{-/-} \leftrightarrow {}^{+/+}$ chimeras ($n = 12$) (Figs. 4B and E, and 5). These defects represented an intermediate phenotype between $ET_A^{+/+} \leftrightarrow {}^{+/+}$ chimeras ($n = 5$) (Fig. 4A and D) and $ET_A^{-/-}$ embryos (Fig. 4C and F). The changes in $ET_A^{-/-} \leftrightarrow {}^{+/+}$ chimeras included maldevelopment of the mandible and tympanic rings and truncation of Meckel's cartilage in its lateral aspects (green arrow in Fig. 4E). An abnormal strut-like structure connected the gonial bone to the pterygoid bone (red arrows in Fig. 4E; see below). Interestingly, morphological changes were also observed in structures that were composed of both wild type and $ET_A^{-/-}$ cells in E13.5 $ET_A^{-/-} \leftrightarrow {}^{+/+}$ chimeras, including the incus and stapes (Fig. 5). Thus, as the percentage of mutant cells increased in $ET_A^{-/-} \leftrightarrow {}^{+/+}$ chimeras, a general shift occurred in craniofacial morphology toward that observed in $ET_A^{-/-}$ embryos.

An interesting change in skull development in $ET_A^{-/-} \leftrightarrow {}^{+/+}$ chimeras was the formation of an abnormal bone strut that formed a bridge between the gonial and pterygoid bones, both of which were malformed (red arrows Fig. 4E). This strut, never observed in $ET_A^{-/-}$ embryos (Fig. 4F), appears similar to struts observed in $Dlx2^{-/-}$ (Qiu et al., 1995, 1997) and $Dlx5^{-/-}$ (Acampora et al., 1999; Depew et al., 1999) embryos, though each has its own unique characteristics.

Contribution of $ET_A^{-/-}$ cells to arch-derived structures in E18.5 chimeras

The above results show that, while malformations were observed in most of the arch-derived craniofacial structures of E18.5 $ET_A^{-/-} \leftrightarrow {}^{+/+}$ chimeras, ventral structures were predominately affected. To determine whether this reflected differences in cell composition of these structures as seen in E13.5 embryos, we examined the contribution of $ET_A^{-/-}$ cells to craniofacial structures of E18.5 $ET_A^{-/-} \leftrightarrow {}^{+/+}$ chimeras using serial frontal sections stained for β-gal activity. As observed at E13.5, $ET_A^{+/+}$ cells were mixed homogeneously throughout craniofacial structures in $ET_A^{+/+} \leftrightarrow {}^{+/+}$ chimeras ($n = 5$) (Fig. 6A and C, and Fig. 7). In contrast, most ventral first arch structures in $ET_A^{-/-} \leftrightarrow {}^{+/+}$ chimeras, including Meckel's cartilage and the mandible, were either composed solely of wild type cells or were absent ($n = 12$) (Fig. 7). More lateral structures, including the incus and stapes, were composed of both wild type and $ET_A^{-/-}$ cells, though these structures were often malformed in $ET_A^{-/-} \leftrightarrow {}^{+/+}$ chimeras containing a large percentage of mutant cells. Thus, ET_A signaling appears to be required cell-autonomously only in ventral arch devel-

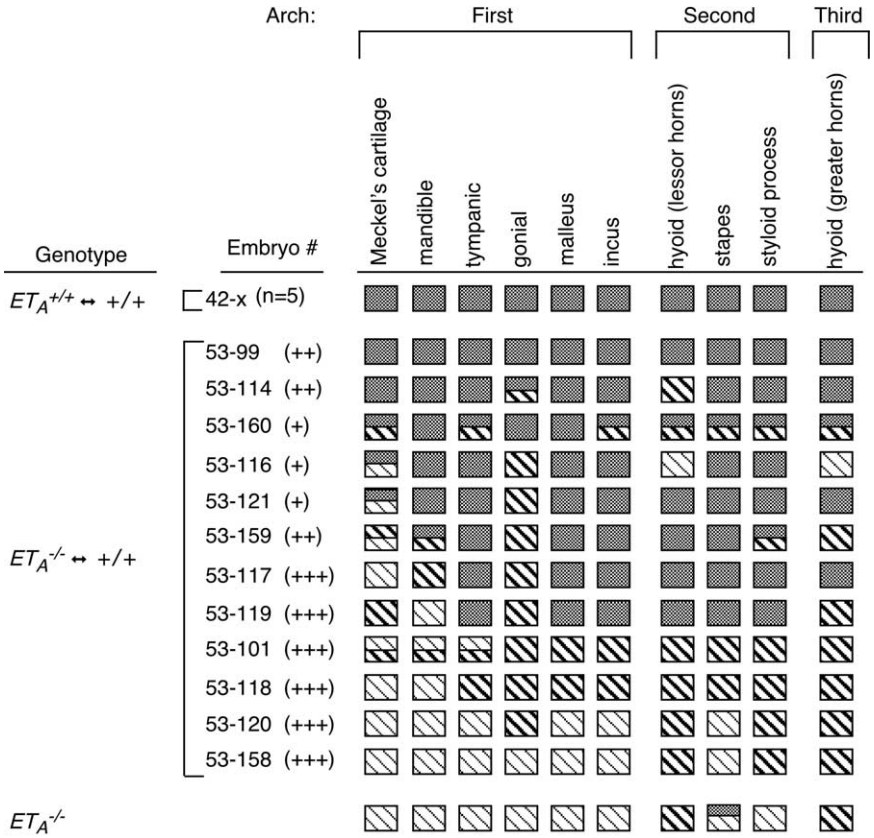

Fig. 5. Analysis of craniofacial structures in E18.5 $ET_A^{+/+} \leftrightarrow +/+$ and $ET_A^{-/-} \leftrightarrow +/+$ chimeras. As described in Fig. 3, the structures examined are listed along the top of the figure, the genotype of the embryos is listed along the left and the relative contribution of injected cells is listed to the right of the embryo number (+ to +++). This analysis is based on alizarin red and alcian blue staining. ■, structures which are present and have normal architecture; ▨, structures which are present but malformed; ▧, structures which are absent. For comparison, observations from E18.5 $ET_A^{-/-}$ embryos (Clouthier et al., 1998) are shown along the bottom. All structures examined in $ET_A^{+/+} \leftrightarrow +/+$ chimeras appear normal. In contrast both ventral structures (Meckel's cartilage through the malleus in the first arch and the lessor horns of the hyoid in the second arch) and lateral structures (incus, stapes and styloid) in $ET_A^{-/-} \leftrightarrow +/+$ chimeras become increasingly malformed as the contribution of injected mutant cells increases, eventually resembling $ET_A^{-/-}$ embryos.

opment. Interestingly, the strut observed on skeletal analysis that connected the gonial bone to the pterygoid bone was composed of both wild type and $ET_A^{-/-}$ cells (data not shown).

Pharyngeal arch artery development in mutant chimeras

$ET_A^{-/-}$ embryos have cardiac outflow tract and septation defects indicative of aberrant cardiac neural crest development (Clouthier et al., 1998). We had previously observed that, while expression of both ET-1 and the ET_A receptor are observed in arch arteries 3, 4, and 6 (Clouthier et al., 1998), defects in $ET_A^{-/-}$ embryos are only observed in arch arteries 4 and 6 (Yanagisawa et al., 1998b). To better understand the basis for these differences, we analyzed the contribution of $ET_A^{-/-}$ cells to the caudal arches and arch artery derivatives in $ET_A^{-/-} \leftrightarrow {}^{+/+}$ chimeras. At E10.0, labeled $ET_A^{+/+}$ cells (blue) in $ET_A^{+/+} \leftrightarrow {}^{+/+}$ chimeras were mixed with wild type cells (pink) in the areas surrounding arch arteries 3, which give rise to the adult right and left common carotid arteries (Fig. 8A). However, in $ET_A^{-/-} \leftrightarrow {}^{+/+}$ chimeras, $ET_A^{-/-}$ cells were excluded from most of arch 3 (Fig. 8B), though as described above, the extent of exclusion decreased as the percentage of mutant cells increased (data not shown). In E13.5 ($n = 6$) and E18.5 ($n = 5$) $ET_A^{+/+} \leftrightarrow {}^{+/+}$ chimeras, $ET_A^{+/+}$ and wild type cells were intermixed around all outflow tract structures, including the ascending aorta (data not shown), common carotid arteries, the aortic arch (derived from left arch artery 4), the junction of the right common carotid with the right subclavian (derived from right arch artery 4), and the ductus arteriosus (derived from left arch artery 6) (Fig. 8C, E, and G, and Fig. 9). In contrast, only wild type cells in E13.5 ($n = 7$) and E18.5 ($n = 7$) $ET_A^{-/-} \leftrightarrow {}^{+/+}$ chimeras were observed in outflow tract and arch artery structures, including the aortic arch and the wall of the ductus arteriosus (*) (Fig. 8D, F, and H, and Fig. 9). $ET_A^{-/-}$ cells were still observed in other structures not normally populated by cardiac neural crest cells, including the descending aorta (data not shown). In one chimera containing a large percentage of $ET_A^{-/-}$ cells, a ventricular septal defect (VSD) and right-sided aortic arch were observed, defects often observed in $ET_A^{-/-}$ embryos.

While these results suggest a cell-autonomous requirement for ET_A signaling by cardiac neural crest cells, the exact mechanism by which loss of ET_A signaling causes specific arch artery defects (Yanagisawa et al., 1998b) remains to be determined.

Discussion

Recent studies by us and others suggest that ET-1/ET_A signaling may provide patterning information in the ventral pharyngeal arches. In this study, we have shown that the development of caudoventral arch-derived elements requires ET_A signaling in a cell-autonomous manner. This requirement does not apply for more lateral arch elements, even though many are malformed or absent in $ET_A^{-/-}$ embryos. These findings illustrate the complexity of intercellular signaling in regional patterning of the pharyngeal arches during craniofacial development.

Segregation of wild type and ET_A mutant cells during arch development

The first observable difference in $ET_A^{-/-} \leftrightarrow {}^{+/+}$ chimeras as compared with control chimeras is the exclusion of $ET_A^{-/-}$ cells from the caudoventral pharyngeal arches at E9.5. $ET_A^{-/-}$ cells are instead observed in the rostrolateral arch, with β-gal staining in this area more intense than in control chimeras. While this could be due to differences in proliferation between wild type and mutant cells, gross changes in the proliferation of $ET_A^{-/-}$ cells were not detected in our preliminary experiments using BrdU incorporation (data not shown). A more likely explanation for this segregation is that mutant cells have a migratory defect and thus accumulate in more lateral areas. This possible requirement for ET_A signaling in crest cell migration is in contrast to previous inferences from $ET_A^{-/-}$ mouse embryos (Clouthier et al., 2000) and *suc/et-1* mutant zebrafish lacking the *ET-1* homolog *sucker* (Miller et al., 2000), in which the expression of molecular markers of migratory cephalic crest cells appeared normal. Further, injection of human ET-1 into *suc/et-1* mutants at a stage after most crest migration is supposedly complete resulted in normal development of ventral arch derivatives (Miller et al., 2000). These findings led the authors to speculate that *suc/et-1* (and thus ET_A receptor signaling), is not necessary for overall crest cell migration. However, our present findings are compatible with a model in which cephalic crest cells require ET_A receptor signaling in a cell-autonomous manner for proper migration. This requirement in not likely absolute, since $ET_A^{-/-}$ cells can reach the ventral arch if the contribution of wild type cells is less than 10%. Using rhombomeric transplantation analysis, Baker et al. (1997) demonstrated that the ability of crest cells to enter and populate an arch is blocked if other crest cells are already present. Thus, if wild type cells arrive in the ventral arch before $ET_A^{-/-}$ cells do, mutant cells would be unable to enter the ventral arch and thus accumulate in the lateral arch.

How could loss of ET_A signaling affect crest migration? Interaction of different cell adhesion molecules on the surface of crest cells is known to affect neural crest cell motility (Xu et al., 2001). It is possible that loss of ET_A signaling disrupts the expression of one or more of these cell adhesion complexes, thus disrupting movement through the arch. That $ET_A^{-/-}$ cells appear to have trouble migrating into the ventral arch might suggest that different "compartments" exist within the arch, each requiring different cell adhesion complexes for traversing. $ET_A^{-/-}$ cells may be able to traverse some regions better than others, possibly explaining why the line delineating wild type and mutant cells in the first and second arches is so sharp (Fig. 1D and F). Determining how loss of ET_A signaling disrupts neural crest development will require further studies.

Cell-autonomous requirement for ET_A signaling in neural crest differentiation

While ET_A signaling may play a role in neural crest cell migration, our data also suggest that it may play a second role in terminal differentiation of crest cells into bone and cartilage structures within the ventral aspects of the first mandibular arch and second arch. In $ET_A^{-/-} \leftrightarrow {}^{+/+}$ chimeras, skeletal structures specifically derived from the ventral mandibular arch, including the mandible and Meckel's

Fig. 6. Development of middle ear structures in E18.5 chimeric embryos. Frontal sections from $ET_A^{+/+}\leftrightarrow+/+$ (A, C) and $ET_A^{-/-}\leftrightarrow+/+$ (B, D) chimeric embryos are shown. Sections are counterstained with eosin (pink). (A, B) Sections through the malleus. In $ET_A^{+/+}\leftrightarrow+/+$ chimeras, $ET_A^{+/+}$ cells (blue) contribute to all of the malleus (m), including the body (b) and manubrium (mb), as well as the incus (i) (A). In $ET_A^{-/-}\leftrightarrow+/+$ chimeras, $ET_A^{-/-}$ cells are only found in the incus and in the perichondral mesenchyme at the articulation of the malleus and incus, but not in the perichondrium surrounding the malleus (B). (C, D) Sections through the incus and stapes (s). Like the pattern observed in $ET_A^{+/+}\leftrightarrow+/+$ chimeras (C), $ET_A^{-/-}$ cells in $ET_A^{-/-}\leftrightarrow+/+$ chimeras are observed in the base, crura, and head of the stapes as well as the incus, excluding the most ventral aspect of the long crus (arrowhead); this area is composed solely of wild type (pink) cells (D). eam, external auditory meatus; otc, otic capsule; ttr, tubotympanic recess.

Fig. 7. Contribution of $ET_A^{+/+}$ and $ET_A^{-/-}$ cells to craniofacial structures of E18.5 chimeric embryos. As described in Fig. 3, the relative contribution of injected cells is listed to the right of the embryo number (+ to +++). ⬛ , structures composed of both injected and wild type cells; ▨ , structures composed of wild type cells only; ▨ , structures that are absent. For comparison, the findings from $ET_A^{-/-}$ embryos are listed at the bottom; ■, structures that are present; □, structures that are malformed or absent. As observed in E13.5 embryos, both ventral and lateral structures in $ET_A^{+/+}\leftrightarrow+/+$ chimeras are composed of both injected and wild type cells. However, ventral structures in $ET_A^{-/-} \leftrightarrow+/+$ chimeras are composed solely of wild type cells or are absent. Lateral structures are composed of both $ET_A^{-/-}$ and wild type cells. $ET_A^{-/-}\leftrightarrow+/+$ chimeras with extensive contribution of $ET_A^{-/-}$ cells have a cleft palate (*)

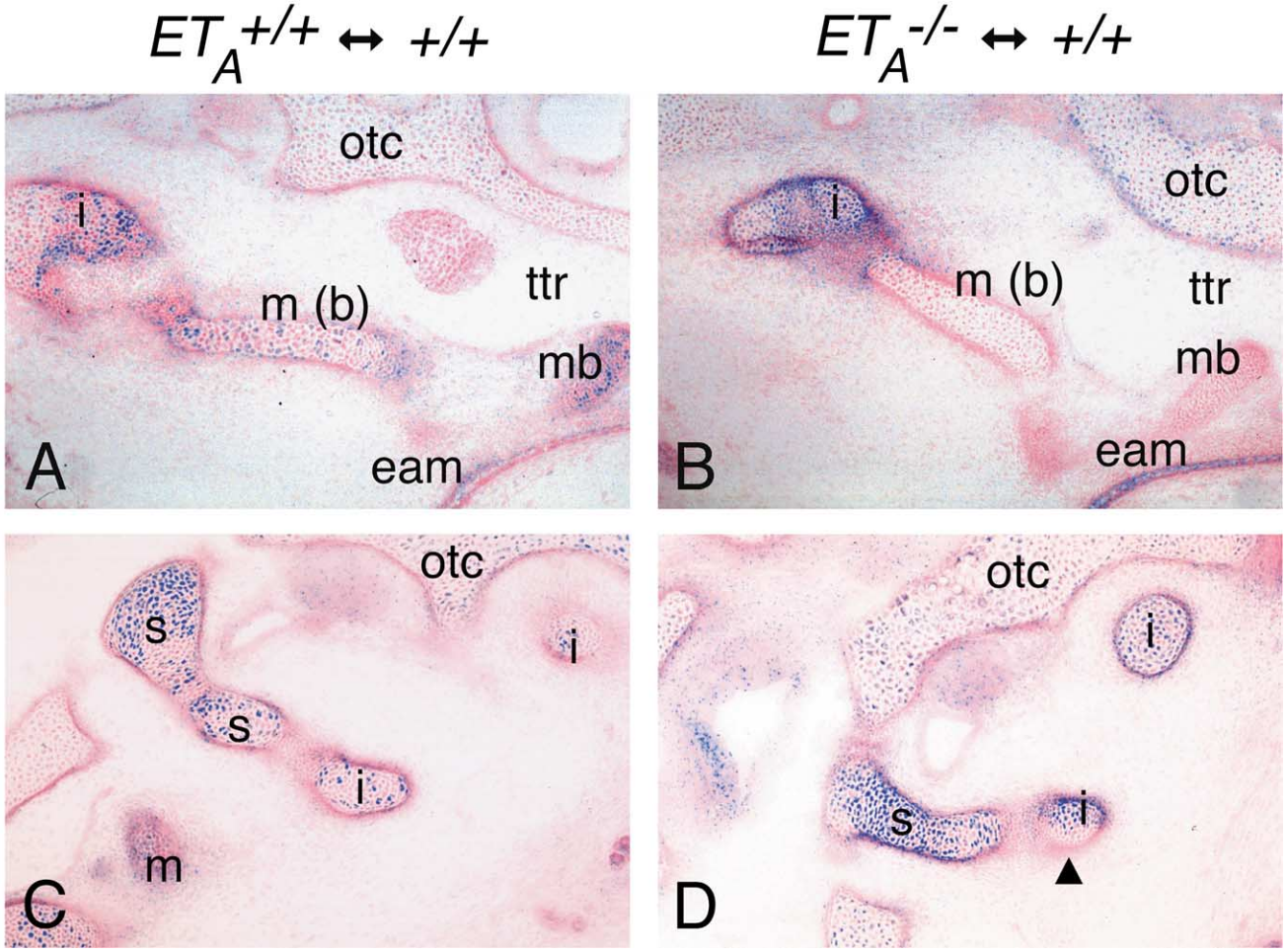
$ET_A^{+/+} \leftrightarrow +/+$
$ET_A^{-/-} \leftrightarrow +/+$
otc
i
m (b)
ttr
mb
eam
A
B
s
m
C
D

6

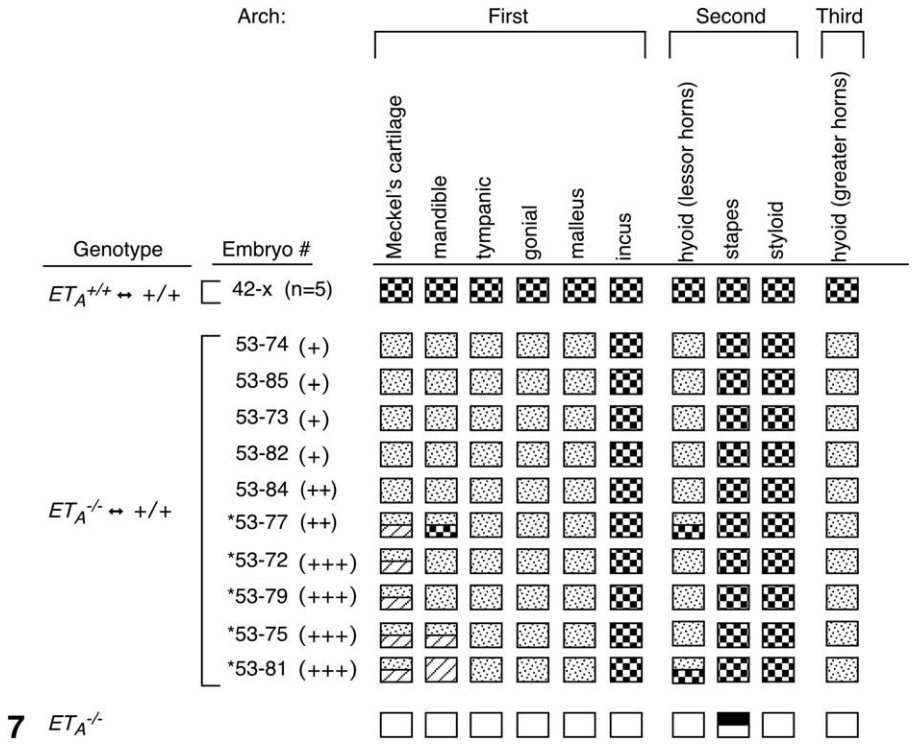
Arch:
First
Second
Third
Meckel's cartilage
mandible
tympanic
gonial
malleus
incus
hyoid (lessor horns)
stapes
styloid
hyoid (greater horns)
Genotype
Embryo #
$ET_A^{+/+} \leftrightarrow +/+$
42-x (n=5)
$ET_A^{-/-} \leftrightarrow +/+$
53-74 (+)
53-85 (+)
53-73 (+)
53-82 (+)
53-84 (++)
*53-77 (++)
*53-72 (+++)
*53-79 (+++)
*53-75 (+++)
*53-81 (+++)
$ET_A^{-/-}$

7

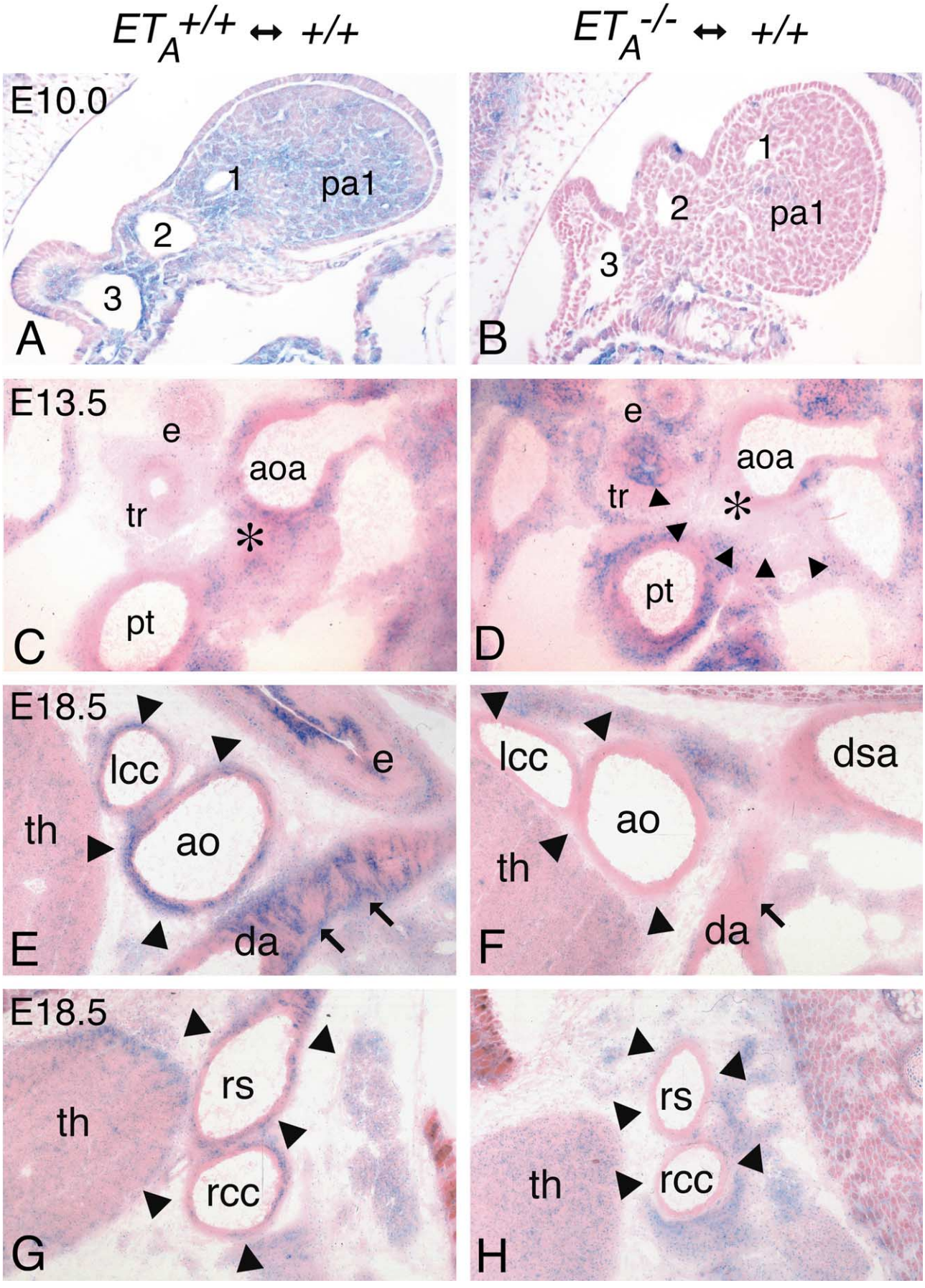
$ET_A^{+/+} \leftrightarrow +/+$
$ET_A^{-/-} \leftrightarrow +/+$
E10.0
1
pa1
2
3
A
1
2
pa1
3
B
E13.5
e
aoa
tr
*
pt
C
e
aoa
tr
*
pt
D
E18.5
lcc
e
th
ao
da
E
lcc
dsa
ao
th
da
F
E18.5
rs
th
rcc
G
rs
th
rcc
H

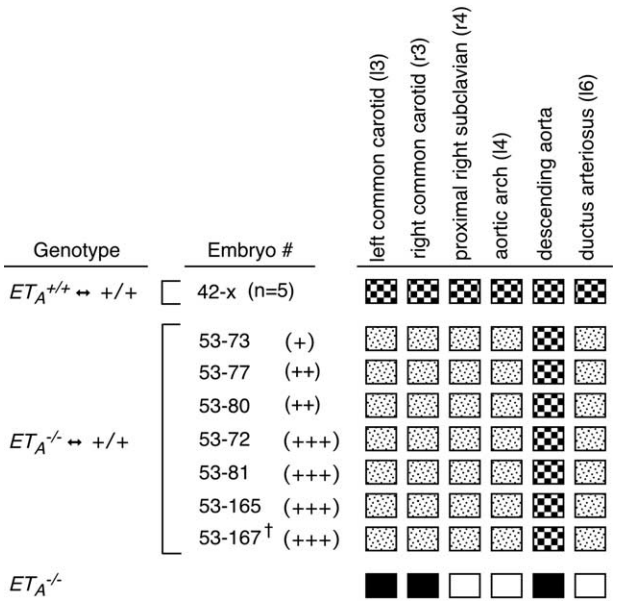

Fig. 9. Contribution of $ET_A^{+/+}$ and $ET_A^{-/-}$ cells to cardiovascular structures of E18.5 chimeric embryos. Arteries of the outflow tract examined are listed along the top; the pharyngeal arch artery origin of each artery is listed in parenthesis. As detailed in Fig. 3, the relative contribution of injected cells is listed to the right of the embryo number (+ to +++). ▩, structures composed of both injected and wild type cells; ▨, structures composed of wild type cells only. Observations from $ET_A^{-/-}$ embryos are listed at the bottom; ■, structures that appear normal; □, structures that are malformed. While $ET_A^{+/+}$ and recipient wild type cells in $ET_A^{+/+} \leftrightarrow +/+$ chimeras are observed in the walls of all arteries, $ET_A^{-/-}$ cells in $ET_A^{-/-} \leftrightarrow +/+$ are only observed in the wall of the descending aorta. The walls of arch artery-derived arteries are composed solely of wild type cells. Notably, $ET_A^{-/-}$ cells are excluded from the walls of the left and right common carotid arteries, though these structures appear normal in $ET_A^{-/-}$ embryos. A ventricular septal defect (†) is only observed in the $ET_A^{-/-} \leftrightarrow +/+$ chimera with the highest contribution of $ET_A^{-/-}$ cells.

cartilage, are composed solely of wild type cells, whereas the incus, a maxillary arch derivative, is composed of both wild type and mutant cells. In $ET_A^{-/-} \leftrightarrow {}^{+/+}$ chimeric embryos containing a large percentage of $ET_A^{-/-}$ cells, $ET_A^{-/-}$ cells do reach the ventral first mandibular arch, yet final structures derived from this region do not form. This indicates that crest-derived ectomesenchymal cells within the mandibular arch have a cell-autonomous requirement for ET_A signaling in order to form bone and cartilage structures. Such a requirement does not exist in the maxillary portion of the first arch, suggesting that ET_A signaling is specifically required for patterning the mandibular arch.

The area within the mandibular arch requiring ET_A signaling for crest cell differentiation appears to coincide with the location of epithelial *ET-1* expression, observed primarily in the caudoventral arch epithelium (Clouthier et al., 1998; Maemura et al., 1996). Thus, proximity to ET-1 may locally lead to ET_A-dependent patterning of caudoventral ectomesenchymal cells. However, it is also possible that neural crest cells of different origins have different requirements for ET_A signaling. Long-term fate maps of neural crest cells in the chick have been used to generate similar maps for the mouse (Kontges and Lumsden, 1996). Comparison of the localization of mandibular abnormalities in $ET_A^{-/-} \leftrightarrow {}^{+/+}$ chimeras with these fate maps illustrate that all affected structures are derived solely or partially from midbrain crest cells (Fig. 10). This suggests that midbrain crest cells may either be preprogrammed to have a specific requirement for ET_A signaling or become ET-1/ET_A-dependent as a result of their final location within the mandibular arch. Since both preprogramming and local patterning by arch-derived factors appear crucial for crest cell development (Trainor and Krumlauf, 2002; Schneider and Helms, 2003), determining which of these aspects relies on ET_A signaling will have to await fate-mapping studies in $ET_A^{-/-}$ embryos.

ET_A signaling and rostrolateral arch development

In $ET_A^{-/-}$ embryos, all three middle ear ossicles (malleus, incus, and stapes) as well as the styloid process are malformed or missing (Clouthier et al., 1998). In this study, we found that the malleus of $ET_A^{-/-} \leftrightarrow {}^{+/+}$ chimeras was composed solely of wild type cells, whereas the incus, stapes, and styloid were each composed of a mixture of both mutant and wild type cells. One interpretation of these

Fig. 8. Development of aortic arch elements in chimeric embryos. Sagittal (E10.0, A, B; and E18.5, E–H) and transverse (E13.5, C, D) sections from $ET_A^{+/+} \leftrightarrow +/+$ (A, C, E, G) and $ET_A^{-/-} \leftrightarrow +/+$ (B, D, F, H) chimeric embryos. Twelve micrometer sections were stained for β-galactosidase activity (blue) and counterstained with eosin (pink). (A, B) Sections through the pharyngeal arch arteries of E10.0 embryos. While $ET_A^{+/+}$ cells (blue) in $ET_A^{+/+} \leftrightarrow +/+$ chimeras are mixed around pharyngeal arch arteries 1, 2, and 3, $ET_A^{-/-}$ cells in $ET_A^{-/-} \leftrightarrow +/+$ chimeras are absent from the arches, with the mesenchyme surrounding the arch arteries instead composed only of wild type cells. Chimerism elsewhere in these embryos was roughly equal. (C, D) Sections through the aortic arch of E13.5 embryos. In $ET_A^{+/+} \leftrightarrow +/+$ chimeras, $ET_A^{+/+}$ cells (blue) are found in the walls of the pulmonary trunk (pt) and the aortic arch (aoa) [proximal to the entrance of the ductus arteriosus (*)] at the junction of the left subclavian artery (C). In $ET_A^{-/-} \leftrightarrow +/+$ chimeras, wild type cells (pink) are not observed in the wall of the ductus arteriosus (arrowheads) and surrounding the aortic arch (D). $ET_A^{-/-}$ cells (blue) are still present in the wall of the pulmonary trunk. (E, F) Sections through the left side of the aortic arch of E18.5 embryos. In $ET_A^{+/+} \leftrightarrow +/+$ chimeras, $ET_A^{+/+}$ cells (blue; arrows and arrowheads) are observed in the walls of the left common carotid artery (lcc; derived from left arch artery 3), aortic arch (ao; derived from left arch artery 4), and the ductus arteriosus (da; derived from left arch artery 6) (E). In $ET_A^{-/-} \leftrightarrow +/+$ chimeras, $ET_A^{-/-}$ cells are absent from the walls of the left common carotid artery, aorta and ductus arteriosus. Vessel walls are composed solely of wild type cells (pink) (F; arrows and arrowheads). (G, H) Sections through the right side of the aortic arch. In $ET_A^{+/+} \leftrightarrow +/+$ chimeras, $ET_A^{+/+}$ cells are observed in the walls of the right common carotid artery (rcc; derived from right aortic arch 3) and the proximal right subclavian artery (rs; derived from right arch artery 4) (arrowheads) (G). In $ET_A^{-/-} \leftrightarrow +/+$ chimeras, $ET_A^{-/-}$ cells appear to be excluded from the walls of the subclavian and common carotid arteries (arrowheads) (H). e, esophagus; pal, pharyngeal arch 1; t, trachea; th, thymus.

results is that the maxillary portion of the first arch (incus) and lateral region of the second arch (stapes and styloid) require ET_A signaling in a non-cell-autonomous manner, indicating the presence of one or more ET_A-dependent paracrine mediators. However, it is also possible that the formation of these elements does not require ET_A signaling, with their malformation in $ET_A^{-/-}$ embryos occurring as a secondary result of the more severe changes in the ventral arch. Tension exerted by neighboring tissues or structures is believed to play a major role in facial development (McGonnell et al., 1998). Loss of the malleus, which disrupts normal articulations with the incus, could in turn disrupt incus development in $ET_A^{-/-}$ embryos. This would explain why the incus becomes deformed as the percentage of $ET_A^{-/-}$ cells in $ET_A^{-/-} \leftrightarrow {}^{+/+}$ chimeras increases, even though the incus is still composed of both wild type and mutant cells.

Abnormal bone development in the skull of $ET_A^{-/-} \leftrightarrow {}^{+/+}$ chimeras

The most frequently observed structural abnormality in the skull of $ET_A^{-/-} \leftrightarrow {}^{+/+}$ chimeras is the presence of a strut-like bone that forms between the gonial and pterygoid bones. This strut is composed of both wild type and $ET_A^{-/-}$ cells, suggesting a change in one or more downstream factors that normally specify development of mesenchymal cells in this region. This strut is never observed in $ET_A^{-/-}$ embryos, possibly reflecting an absence of precursor cells in mutant embryos due to mesenchymal cell apoptosis occurring earlier in development (Clouthier et al., 2000). Cell number dependency has been hypothesized to occur during tympanic ring formation in $Gsc^{-/-} \leftrightarrow {}^{+/+}$ chimeras (Rivera-Perez et al., 1999). Mesenchymal bone struts are also observed in $Dlx2^{-/-}$ (Qiu et al., 1995, 1997) and $Dlx5^{-/-}$ (Acampora et al., 1999; Depew et al., 1999) embryos. Since the expression of several *Dlx* genes requires ET_A signaling (Clouthier et al., 2000, Charité et al., 2001, and data not shown), it is possible that strut formation in these different mouse mutants results from the loss of a common mesenchymal factor(s) that either induce or repress alternative developmental pathways (possibly Dlx factors themselves). Loss of *Dlx*5 and *Dlx*6 disrupts patterning of the mandibular arch, resulting in an apparent homeotic transformation of mandibular arch structures into maxillary arch structures (Beverdam et al., 2002; Depew et al., 2002). Since much of the mandibular arch-derived bone in $ET_A^{-/-}$ mutant embryos is absent or severely deformed, it is difficult to determine whether a similar homeotic transformation is present. Strategies that produce a more restricted loss of ET_A receptor function will be required to fully understand the role(s) of ET_A signaling in patterning the mandibular arch.

Cell-autonomous action of ET_A during aortic arch development

We previously demonstrated that the development of arch 4 and 6 derivatives is disrupted in $ET_A^{-/-}$ embryos (Clouthier et al., 1998; Yanagisawa et al., 1998b). In this study, we found that $ET_A^{-/-}$ cells are excluded from caudal arches 3, 4, and 6 in $ET_A^{-/-} \leftrightarrow {}^{+/+}$ chimeras, resulting in the walls of arch arteries 3, 4, and 6 derivatives being composed almost entirely of wild type cells. As described above for cephalic neural crest development, these findings suggest that ET_A signaling is required in a cell-autonomous manner for some aspect of cardiac neural crest development, regardless of the arch artery segment with which they are associated. It is interesting to note that outflow tract defects were only observed in 14% of E18.5 $ET_A^{-/-} \leftrightarrow {}^{+/+}$ chimeras examined, suggesting that the number of wild type cardiac neural crest cells necessary for correct arch artery remodeling may be quite small.

As described above for cephalic neural crest development, the lack of ET_A mutant cells in the arch artery walls of mutant chimeras may result from a defect in cardiac crest cell migration (Brault et al., 2001; Huang et al., 1998; Waldo et al., 1999). Aberrant cardiac crest cell migration is believed to be the cause of outflow tract defects in $Pax3^{-/-}$ mice, in which the sixth arch-derived ductus arteriosus is commonly affected (Conway et al., 1997). However, more recent studies in which cardiac neural crest cells in $Pax3^{-/-}$ embryos have been fate mapped suggest that *Pax3*, though not essential for migration, is required for more subtle aspects of crest cell development, possibly including the final targeting of crest cells to the outflow tract (Epstein et al., 2000). We previously demonstrated that expression of *CRABP1*, a cardiac neural crest marker, was not grossly altered in $ET_A^{-/-}$ embryos, suggesting that cardiac neural crest cell migration is unaffected in $ET_A^{-/-}$ embryos (Yanagisawa et al., 1998b). However, as observed in *Pax3* mutant embryos, it is possible that loss of ET_A signaling affects the eventual targeting or survival of cardiac crest cells, rather than their migration away from the neural tube. Determining whether crest cell migration is affected in $ET_A^{-/-}$ embryos will require extensive cardiac neural crest fate mapping as well as determining the timing of ET_A receptor function.

Marked phenotypic similarities between $ET_A^{-/-}$ embryos and mouse models of DiGeorge syndrome (Jerome and Papaioannou, 2001; Lindsay et al, 2001; Merscher et al., 2001; Kochilas et al., 2002; Vitelli et al., 2002) suggest that ET_A signaling may function within the same genetic pathway involving *Tbx1* and other gene(s) within the DiGeorge-syntenic region. Further analyses of the role of endothelin-mediated paracrine signaling in craniofacial and cardiovascular development may lead to a better understanding of the molecular pathogenesis of DiGeorge syndrome.

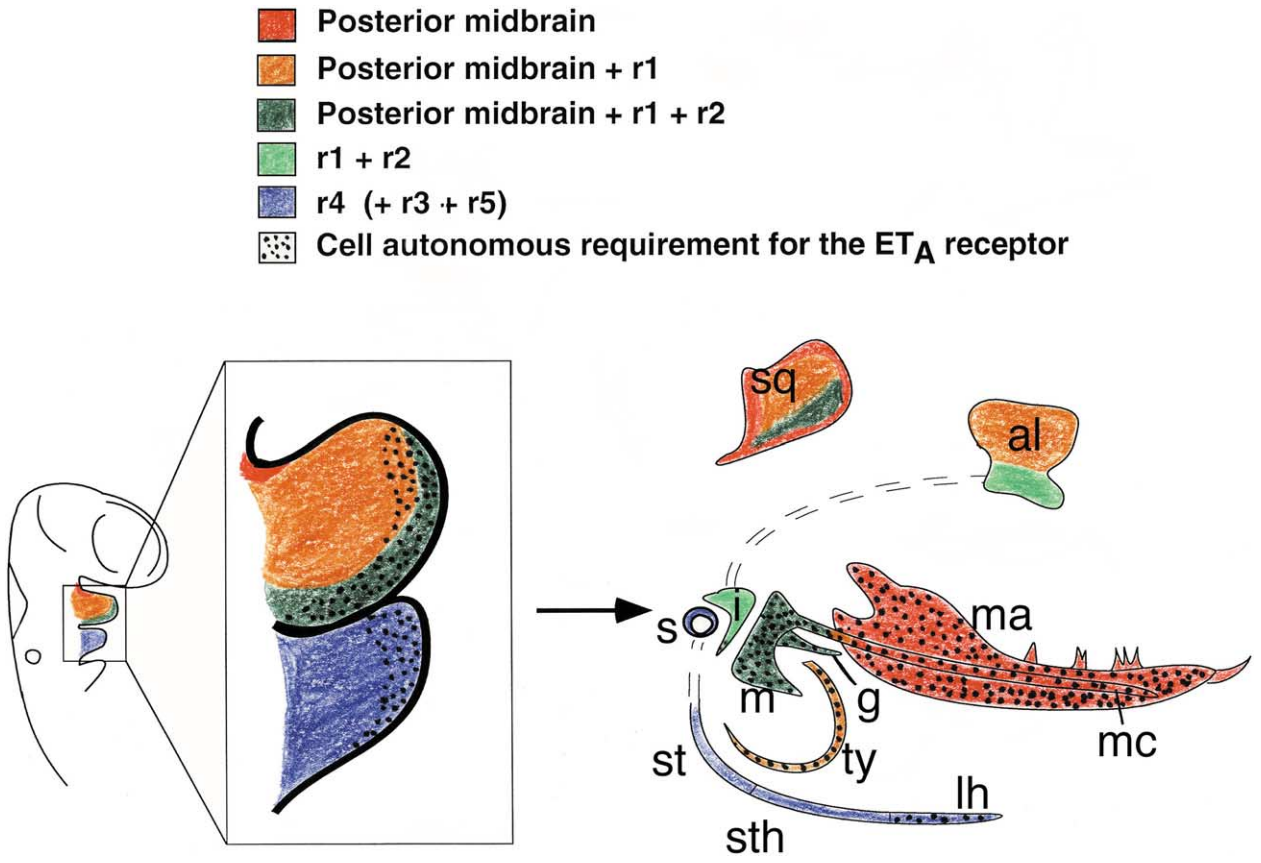

Fig. 10. Schematic representation of the cell-autonomous requirement of ET_A signaling during pharyngeal arch development. The left side of the figure illustrates that cephalic neural crest cells arising from the midbrain and hindbrain (color coded, matching the original color scheme used by Kontges and Lumsden, 1996) and populating pharyngeal arches one and two (enlarged in box) give rise to most craniofacial structures (Kontges and Lumsden, 1996). Arch areas that are dotted represent populations of crest-derived ectomesenchymal cells believed to have a cell-autonomous requirement for ET_A receptor signaling. In mutant chimeras, skull structures arising from these populations (stipled on right side of figure) are either composed solely of wild type cells or are missing. Notably, structures that are composed of neural crest cells originating in the posterior midbrain appear to be most severely affected. al, alisphenoid bone; g, gonial bone; i, incus; lh, lessor horns of the hyoid bone; m, malleus; ma, mandible; mc, Meckel's cartilage; s, stapes; sq, squamosal bone; st, styloid; sth, stylohyoid ligament; t, tympanic ring.

Acknowledgments

We thank Richard R. Behringer for critically reading this manuscript and helpful discussions. We would also like to thank Shelley Dixon, Sahar Seyedkalal, Shanna D. Maika, and Elizabeth Loomis for technical help. M.Y. is an Investigator of the Howard Hughes Medical Institute. D.E.C. was a fellow in the Division of Molecular Cardiology and was supported by NIH Training Grant HL07360. This work was supported in part by research grants from the Perot Family Foundation and W.M. Keck Foundation.

References

Acampora, D., Merlo, G.R., Paleari, L., Zerega, B., Postiglione, M.P., Mantero, S., Bober, E., Barbieri, O., Simeone, A., Levi, G., 1999. Craniofacial, vestibular and bone defects in mice lacking the *Distal-less*-related gene *Dlx5*. Development 126, 3795–3809.

Baker, C.V.H., Bonner-Fraser, M., Le Douarin, N.M., Teillet, M.-A., 1997. Early- and late-migrating neural crest cell populations have equivalent developmental potential in vivo. Development 124, 3077–3087.

Beverdam, A., Merlo, G.R., Paleari, L., Mantero, S., Genova, F., Barbieri, O., Janvier, P., Levi, G., 2002. Jaw transformation with gain or symmetry after *Dlx5/Dlx 6* inactivation: mirror of the past. Genesis 34, 221–227.

Brault, V., Moore, R., Kutsch, S., Ishibashi, M., Rowitch, D.H., McMahon, A.P., Sommer, L., Roussadia, O., Kemler, R., 2001. Inactivation of the β-catenin gene by *Wnt1-Cre*-mediated deletion results in dramatic brain malformation and failure of craniofacial development. Development 128, 1253–1264.

Chai, Y., Jiang, X., Ito, Y., Bringas, P., Han, J., Rositch, D.H., Soriano, P., McMahon, A.P., Sucov, H.M., 2000. Fate of the mammalian cranial neural crest during tooth and mandibular morphogenesis. Development 127, 1671–1679.

Charité, J., McFadden, D.G., Merlo, G.R., Levi, G., Clouthier, D.E., Yanagisawa, M., Richardson, J.A., Olson, E.N., 2001. Role of Dlx6 in regulation of an endothelin-1-dependent, *dHAND* branchial arch enhancer. Genes Dev. 15, 3039–3049.

Chen, Z.-F., Behringer, R.R., 1995. *twist* is required in head mesenchyme for cranial neural tube morphogenesis. Genes Dev. 9, 686–699.

Clouthier, D.E., Hosoda, K., Richardson, J.A., Williams, S.C., Yanagisawa, H., Kuwaki, T., Kumada, M., Hammer, R.E., Yanagisawa, M., 1998. Cranial and cardiac neural crest defects in endothelin-A receptor-deficient mice. Development 125, 813–824.

Clouthier, D.E., Williams, S.C., Yanagisawa, H., Wieduwilt, M., Richardson, J.A., Yanagisawa, M., 2000. Signaling pathways crucial for craniofacial development revealed by endothelin-A receptor-deficient mice. Dev. Biol. 217, 10–24.

Conway, S.J., Henderson, D.J., Copp, A.J., 1997. *Pax3* is required for cardiac neural crest migration in the mouse: evidence from the *splotch* *(Sp^{2H})* mutant. Development 124, 505–514.

Creazzo, T.L., Godt, R.E., Leatherbury, L., Conway, S.J., Kirby, M.L., 1998. Role of cardiac neural crest cells in cardiovascular development. Annu. Rev. Physiol. 60, 267–286.

Depew, M.J., Liu, J.K., Long, J.E., Presley, R., Meneses, J.J., Pedersen, R.A., Rubenstein, J.L.R., 1999. *Dlx5* regulates regional development of the branchial arches and sensory capsules. Development 126, 3831–3846.

Depew, M.J., Lufkin, T., Rubenstein, J.L.R., 2002. Specification of jaw subdivisions by *Dlx* genes. Science 298, 381–385.

Epstein, J.A., Li, J., Land, D., Chen, F., Brown, C.B., Jin, F., Lu, M.M., Thomas, M., Liu, E., Wessels, A., Lo, C.W., 2000. Migration of cardiac neural crest cells in *Splotch* embryos. Development 127, 1869–1878.

Friedrich, G., Soriano, P., 1991. Promoter traps in embryonic stem cells: a genetic screen to identify and mutate developmental genes in mice. Genes Dev. 5, 1513–1525.

Huang, G.Y., Wessels, A., Smith, B.R., Linask, K.K., Ewart, J.L., Lo, C.W., 1998. Alteration of connexin 43 gap junction gene dosage impairs conotruncal heart development. Dev. Biol. 198, 32–44.

Jerome, L.A., Papaioannou, V.E., 2001. DiGeorge syndrome phenotype in mice mutant for the T-box gene, *Tbx1*. Nat. Genet. 27, 286–291.

Kirby, M.L., Gale, T.F., Stewart, D.E., 1983. Neural crest cells contribute to aorticopulmonary septation. Science 220, 1059–1061.

Kirby, M.L., Stewart, D.E., 1983. Neural crest origin of cardiac ganglion cells in the chick embryo: identification and extirpation. Dev. Biol. 97, 433–443.

Kirby, M.L., Turnage, K.L., Hays, B.M., 1985. Characterization of conotruncal malformations following ablation of "cardiac" neural crest. Anat. Rec. 213, 87–93.

Kochilas, L., Merscher-Gomez, S., Lu, M.M., Potluri, V., Liao, J., Kucherlapati, R., Morrow, B., Epstein, J.A., 2002. The role of neural crest during cardiac development in a mouse model of DiGeorge syndrome. Dev. Biol. 251, 157–166.

Kontges, G., Lumsden, A., 1996. Rhombencephalic neural crest segmentation is preserved throughout craniofacial ontogeny. Development 122, 3229–3242.

Kurihara, Y., Kurihara, H., Suzuki, H., Kodama, T., Maemura, K., Nagai, R., Oda, H., Kuwaki, T., Cao, W.-H., Kamada, N., et al., 1994. Elevated blood pressure and craniofacial abnormalities in mice deficient in endothelin-1. Nature 368, 703–710.

Le Douarin, N.M., Ziller, C., Couly, G.F., 1993. Patterning of neural crest derivatives in the avian embryo: in vivo and in vitro studies. Dev. Biol. 159, 24–49.

Le Lievre, C.S., Le Douarin, N.M., 1975. Mesenchymal derivatives of the neural crest: analysis of chimaeric quail and chick embryos. J. Embryol. Exp. Morphol. 34, 125–154.

Lindsay, E.A., Vitelli, F., Su, H., Morishima, M., Huynh, T., Pramparo, T., Jurecic, V., Ogunrinu, G., Sutherland, H.F., Scambler, P.J., Bradley, A., Baldini, A., 2001. *Tbxl* haploinsufficiency in the DiGeorge syndrome region causes aortic arch defects in mice. Nature 410, 97–101.

Lumsden, A., Sprawson, N., Graham, A., 1991. Segmental origin and migration of neural crest cells in the hindbrain region of the chick embryo. Development 113, 1281–1291.

Maemura, K., Kurihara, H., Kurihara, Y., Oda, H., Ishikawa, T., Copeland, N.G., Gilbert, D.J., Jenkins, N.A., Yazaki, Y., 1996. Sequence analysis, chromosomal location, and developmental expression of the mouse preproendothelin-1 gene. Genomics 31, 177–184.

McGonnell, I.M., Clarke, J.D.W., Tickle, C., 1998. Fate map of the developing chick face: analysis of expansion of facial primordia and establishment of the primary palate. Dev. Dyn. 212, 102–118.

Merscher, S., Funke, B., Epstein, J.A., et al., 2001. *TBX1* is responsible for cardiovascular defects in velo-cardio-facial/DiGeorge syndrome. Cell 104, 619–629.

Miller, C.T., Schilling, T.F., Lee, K.-H., Parker, J., Kimmel, C.B., 2000. *sucker* encodes a zebrafish Endothelin-1 required for ventral pharyngeal arch development. Development 127, 3815–3838.

Noden, D.M., 1983. The role of the neural crest in patterning of avian cranial skeletal, connective, and muscle tissues. Dev. Biol. 96, 144–165.

Qiu, M., Bulfone, A., Ghattas, I., Meneses, J.J., Christensen, L., Sharpe, P.T., Presley, R., Pedersen, R.A., Rubenstein, J.L.R., 1997. Role of the Dlx homeobox genes in proximodistal patterning of the branchial arches: Mutations of Dlx-1, Dlx-2, and Dlx-1 and -2 alter morphogenesis of proximal skeletal and soft tissue structures derived from the first and second arches. Dev. Biol. 185, 165–184.

Qiu, M., Bulfone, A., Martinez, S., Meneses, J.J., Shimamura, K., Pedersen, R.A., Rubenstein, J.L.R., 1995. Null mutation of *Dlx-2* results in abnormal morphogenesis of proximal first and second branchial arch derivatives and abnormal differentiation in the forebrain. Genes Dev. 9, 2523–2538.

Rivera-Perez, J.A., Wakamiya, M., Behringer, R.R., 1999. *Goosecoid* acts cell autonomously in mesenchyme-derived tissues during craniofacial development. Development 126, 3811–3821.

Robertson, E.J., 1987. Embryo-derived stem cell lines, in: Robertson, E.J. (Ed.), Teratocarcinomas and Embryonic Stem Cells: A Practical Approach, IRL Press Limited, Oxford, pp. 71–112.

Rossant, J., Spence, A., 1998. Chimeras and mosaics in mouse mutant analysis. Trends Genet. 14, 358–363.

Schneider, R.A., Helms, J.A., 2003. The cellular and molecular origins of beak morphology. Science 299, 565–568.

Serbedzija, G.N., Bronner-Fraser, M., Fraser, S.E., 1992. Vital dye analysis of cranial neural crest cell migration in the mouse embryo. Development 116, 297–307.

Trainor, P., Krumlauf, R., 2000. Plasticity in mouse neural crest cells reveals a new patterning role for cranial mesoderm. Nat. Cell Biol. 2, 96–102.

Tran, C.M., Sucov, H.M., 1998. The *RXRα* gene functions in a non-cell-autonomous manner during mouse cardiac morphogenesis. Development 125, 1951–1956.

Tucker, S.A., Yamada, G., Grigoriou, M., Pachnis, V., Sharpe, P.T., 1999. Fgf-8 determines rostral-caudal polarity in the first branchial arch. Development 126, 51–61.

Vitelli, F., Morishima, M., Taddei, I., Lindsay, E.A., Baldini, A., 2002. *Tbx1* mutation causes multiple cardiovascular defects and disrupts neural crest and cranial nerve migratory pathways. Hum. Mol. Genet. 11, 915–922.

Waldo, K.L., Lo, C.W., Kirby, M.L., 1999. Connexin 43 expression reflects neural crest patterns during cardiovascular development. Dev. Biol. 208, 307–323.

Xu, X., Li, W.E.I., Huang, G.Y., Meyer, R., Chen, T., Luo, Y., Thomas, M.P., Radice, G.L, Lo, C.W., 2001. Modulation of mouse neural crest cell motility by N-cadherin and connexin 43 gap junctions. J. Cell Biol. 154, 217–22.

Yanagisawa, H., Yanagisawa, M., Kapur, R.P., Richardson, J.A., Williams, S.C., Clouthier, D.E., de Wit, D., Emoto, N., Hammer, R.E., 1998a. Dual genetic pathways of endothelin-mediated intercellular signaling revealed by targeted disruption of endothelin converting enzyme-1 gene. Development 125, 825–836.

Yanagisawa, H., Hammer, R.E., Richardson, J.A., Williams, S.C., Clouthier, D.E., Yanagisawa, M., 1998b. Role of endothelin-1/endothelin-A receptor-mediated signaling pathway in the aortic arch patterning in mice. J. Clin. Invest. 102, 22–33.

Zambrowicz, B.P., Zimmermann, J.W., Harendza, C.J., Simpson, E.M., Page, D.C., Brinster, R.L., Palmiter, R.D., 1994. Expression of a mouse Zfy-1/lacZ transgene in the somatic cells of the embryonic gonad and germ cells of the adult testis. Development 120, 1549–1559.